https://doi.org/10.5194/acp-2022-175
Preprint. Discussion started: 4 April 2022

Atmospheric Chemistry and Physics Discussions
Open Access

Fire-climate interactions through aerosol radiative effect in a global chemistry-climate-vegetation model

Chenguang Tian[1, 2], Xu Yue[1], Jun Zhu[1], Hong Liao[1], Yang Yang[1], Yadong Lei[3], Xinyi Zhou[1], Hao Zhou[2], Yimain Ma[2], Yang Cao[2]

[1] Jiangsu Key Laboratory of Atmospheric Environment Monitoring and Pollution Control, Collaborative Innovation Center of Atmospheric Environment and Equipment Technology, School of Environmental Science and Engineering, Nanjing University of Information Science & Technology (NUIST), Nanjing, 210044, China

[2] Climate Change Research Center, Institute of Atmospheric Physics, Chinese Academy of Sciences, Beijing, 100029, China

[3] State Key Laboratory of Severe Weather & Key Laboratory of Atmospheric Chemistry of CMA, Chinese Academy of Meteorological Sciences, Beijing, 100081, China

Corresponding author: Xu Yue (Email: yuexu@nuist.edu.cn)

https://doi.org/10.5194/acp-2022-175
Preprint. Discussion started: 4 April 2022

Atmospheric Chemistry and Physics Discussions
Open Access EGU

Abstract

Fire emissions influence radiation, climate, and ecosystems through aerosol radiative effects. Meanwhile, these environmental perturbations can feed back to affect fire emissions. However, the magnitude of such fire-climate interactions remains unclear on the global scale. Here, we quantify the impacts of fire aerosols on climate through direct, indirect, and albedo effects based on the two-way simulations using a well-established chemistry-climate-vegetation model. Globally, fire emissions cause a reduction of -0.57 W m^{-2} in net radiation at the top of atmosphere with dominant contributions by aerosol indirect effect (AIE). Consequently, surface air temperature decreases by 0.06°C with coolings of >0.25°C over eastern Amazon, western U.S., and boreal Asia. Both aerosol direct effect (ADE) and AIE contribute to such cooling while the aerosol albedo effect (AAE) exerts an offset warming especially at high latitudes. Land precipitation decreases by 0.018 mm $month^{-1}$ mainly due to the inhibition in central Africa by AIE. Such rainfall deficit further reduces regional leaf area index (LAI) and lightning ignitions, leading to changes in fire emissions. Globally, fire emissions reduce by 2%-3% because of the fire-induced changes in humidity, lightning, and LAI. The fire-climate interactions may cause larger perturbations to climate systems with likely more fires under global warming.

Short summary

We quantify the impacts of fire aerosols on climate through direct, indirect, and albedo effects. We find global fire aerosols cause a cooling of surface air temperature and an inhibition of precipitation. These climatic perturbations further reduce regional leaf area index and lightning ignitions, both of which are not beneficial for fire emissions. By considering the feedback of fire aerosols on humidity, lightning, and LAI, we predict a slight reduction in fire emissions.

Keywords: Fire emissions; fire-climate interaction; radiative effect; climate feedback; ModelE2-YIBs model

https://doi.org/10.5194/acp-2022-175
Preprint. Discussion started: 4 April 2022

Atmospheric Chemistry and Physics Discussions

1 Introduction

Fire occurs all year round in both hemispheres, burning about 1% of the Earth's surface and emitting roughly 2–3 Pg (=10^{15} g) carbon into atmosphere every year (Van Der Werf et al., 2017). Fire activities are strongly influenced by fuel availability, ignition/suppression, and climate conditions (Flannigan et al., 2009). The fuel type, continuity, and amount affect fire occurrence and spread probability (Flannigan et al., 2013). Lightning discharge is the most important natural source of fire ignition (Macias Fauria and Johnson, 2006). Human activities affect fire patterns by adding ignition sources or by suppressing processes (Andela et al., 2017). Compared to the above factors, climate shows a more dominant role in modulating fire activities through the changes of fuel moisture and spread conditions (Flannigan and Harrington, 1988).

Fire exerts prominent impacts on Earth systems and human society through various processes. Biomass burning emits a large amount of trace gases and aerosol particles into the troposphere, affecting air quality at the local and downwind regions (Yue and Unger, 2018). *In situ* observations showed that about one-third of the background particles in the free troposphere of North America were originated from biomass burning (Hudson et al., 2004). Extremely intense fires can even inject aerosols into stratosphere, where the particles were transported globally (Yu et al., 2019). Fire-induced air pollution can reduce global terrestrial productivity of unburned forests (Yue and Unger, 2018), leading to weakened carbon uptake by ecosystems. The global transport of fire air pollution also causes large threats to public health by increasing the risks of diseases and mortality (Liu et al., 2015). It is estimated that fire-induced particulate matter causes more than 33,000 deaths globally each year (Chen et al., 2021).

Aerosols from fires can cause substantial feedbacks to climate owing to their different optical and chemical properties (Xu et al., 2021). First, aerosols scatter and/or absorb solar radiation through aerosol direct effect (ADE), leading to altered energy budget and climate variables (Carslaw et al., 2010). There is no agreement on the sign of ADE of biomass burning aerosols at the global scale. Some studies (Heald et al., 2014; Veira et al., 2015; Zou et al., 2020) predicted positive forcing while others (Ward et al., 2012; Jiang et al., 2016; Grandey et al., 2016) yielded negative forcing (−0.2 to 0.2 W m^{-2}), mainly because of the large uncertainties in the absorption of fire-emitted black carbon (BC) (Carslaw et al., 2010; Ipcc, 2014). Second, aerosols can serve as cloud condensation nuclei (CCN) or ice nuclei to affect the microphysical properties of cloud. Such aerosol indirect

https://doi.org/10.5194/acp-2022-175
Preprint. Discussion started: 4 April 2022

Atmospheric Chemistry and Physics Discussions

effect (AIE) further influences climate system through the changes of cloud albedo and lifetime (Twomey, 1974; Albrecht, 1989). Globally, fire aerosols account for ~30% of the total CCN (Andreae et al., 2004) and the overall negative AIE of fire aerosol is stronger than the ADE in magnitude (Liu et al., 2014; Ward et al., 2012; Jiang et al., 2016). Third, deposition of fire-emitted BC aerosols reduces surface albedo and promotes ice/snow melting, which is called aerosol-albedo effect (AAE) (Hansen and Nazarenko, 2004; Warren and Wiscombe, 1980). Compared with other two effects, the AAE shows more regional characteristics (Kang et al., 2020). These fire-induced disturbance in radiative fluxes further alter meteorological and hydrologic variables, which in turn affect fire activities through the changes in fuel moisture and weather conditions.

The two-way interactions between fire and climate have not been fully assessed. While observations revealed fire-induced perturbations to regional climate (Bali et al., 2017; Zhuravleva et al., 2017), its feedback to fire activities are difficult to be isolated from the influences of background climate. Models provide unique tools to explore fire-climate interactions especially at the regional to global scales. However, fire-climate interactions are not routinely included in most of Earth system models. The IPCC sixth assessment report (AR6) did not provide a quantitative assessment of fire-climate feedback as well (Ipcc, 2021). In this study, we explore the impacts of fire aerosols on climate and the consequent feedbacks to fire emissions by using a well-established fire parameterization coupled to a chemistry-climate-vegetation model ModelE2-YIBs (Yue and Unger, 2015). The main objectives are (1) to isolate the radiative effects of fire aerosols through ADE, AIE, and AAE processes and (2) to quantify the feedback of fire-induced climate effects to fire emissions and air pollutants.

2 Data and methods

2.1 Data

We use the emissions of BC and organic carbon (OC) aerosols from Global Fire Emission Database version 4.1s (GFED4.1s) to validate the simulated fire emissions. The GFED4.1s provides monthly fire emission fluxes of various air pollutants based on satellite retrieval of area burned from the Moderate Resolution Imaging Spectroradiometer (MODIS) (Van Der Werf et al., 2017). Area burned in GFED4.1s is mainly derived from the MODIS burned area product (Giglio et al., 2013), taking into account "small" fires outside the burned area maps based on active fire detections

https://doi.org/10.5194/acp-2022-175
Preprint. Discussion started: 4 April 2022

(Randerson et al., 2012). The gridded fire emission dataset has a spatial resolution of 0.25 °×0.25 ° and is available for every month from July 1997. To estimate anthropogenic ignition and suppression effects, we use a downscaled population density dataset from Gao (2017, 2020). Monthly sea surface temperature (SST) and sea ice (SIC) obtained from Hadley Centre Sea Ice and Sea Surface Temperature (HadISST) dataset (Rayner et al., 2003) are used as the boundary conditions for the climate model.

2.2 ModelE2-YIBs model

The chemistry-climate-vegetation model ModelE2-YIBs is used to simulate the two-way coupling between fire aerosols and climate systems. The ModelE2-YIBs is composed of the NASA Goddard Institute for Space Studies (GISS) ModelE2 model (Schmidt et al., 2014) and the Yale Interactive terrestrial Biosphere Model (YIBs) (Yue and Unger, 2015). The GISS ModelE2 is a global climate-chemistry model with a horizontal resolution of 2° × 2.5° latitude by longitude and 40 vertical layers extending to the stratosphere (0.1hPa). The model simulates gas-phase chemistry, aerosols, and interactions among them. Well-established schemes are used to calculate direct (Koch et al., 2006), indirect (Menon et al., 2008; Menon et al., 2010), and albedo (Warren and Wiscombe, 1980, 1985) effects of aerosol species on the climate. It has been extensively evaluated for meteorological and chemical variables against observations, reanalysis products and other models, and widely used for studies of climate systems, atmospheric components, and their interactions (Schmidt et al., 2014).

YIBs is a process-based vegetation model dynamically simulates tree growth and terrestrial carbon fluxes with prescribed fractions of nine plant functional types (PFTs), including deciduous broadleaf forest, evergreen needleleaf forest, evergreen broadleaf forest, tundra, shrubland, C_3/C_4 grassland, and C_3/C_4 cropland. Essential biological processes such as photosynthesis, phenology, autotrophic and heterotrophic respiration are considered and parameterized using the state-of-the-art schemes (Yue and Unger, 2015). Simulated tree height, phenology, and leaf area index (LAI) agree well with site-level observations and/or satellite retrievals (Yue and Unger, 2015). The YIBs model joined the dynamic global vegetation model inter-comparison project TRENDY and showed reasonable performance of carbon fluxes against available observations (Friedlingstein et al., 2020). By incorporating YIBs into ModelE2, the new coupled model ModelE2-YIBs can simulate

https://doi.org/10.5194/acp-2022-175
Preprint. Discussion started: 4 April 2022

Atmospheric Chemistry and Physics
Discussions

interactions between terrestrial ecosystems and climate systems through the exchange of water and energy fluxes, and chemical components (Yue and Unger, 2015; Yue et al., 2017).

2.3 Fire parameterization

We implemented the active global fire parameterization from Pechony and Shindell (2009) into ModelE2-YIBs model. The parameterization considers key fire-related processes including fuel flammability, lightning and human ignitions, and human suppressions. Flammability is a unitless metric indicating conditions favorable for fire occurrence, and is calculated using vapor pressure deficit (VPD, hPa), precipitation (R, day mm^{-1}), and LAI (m^2 m^{-2}) as follows:

$$\mathrm{Flam} = \mathrm{VPD} \times \mathrm{LAI} \times e^{-c_R \times R} \quad (1)$$

Here, LAI represents vegetation density and is dynamically calculated by YIBs model. c_R is a constant set to 2. VPD is a vital indicator of flammability conditions:

$$\mathrm{VPD} = e_s \times \left(1 - \frac{\mathrm{RH}}{100}\right) \quad (2)$$

where e_s is the saturation vapor pressure and RH is surface relative humidity. e_s can be calculated by Goff-Gratch equation:

$$e_s = e_{st} \times 10^Z \quad (3)$$

where e_{st} is 1013.246 hPa and

$$Z = a \times \left(\frac{T_s}{T} - 1\right) + b \times \log\frac{T_s}{T} + c \times \left(10^{d\left(1-\frac{T_s}{T}\right)} - 1\right) + f \times \left(10^{h\left(\frac{T_s}{T}-1\right)} - 1\right) \quad (4)$$

Here, a, b, c, d, f and h are constants set to -7.90298, 5.02808, -1.3816×10^{-7}, 11.344, 8.1328×10^{-3} and -3.49149, respectively. T_s is boiling point of water and equal to 373.16 K.

Natural and anthropogenic ignitions determine whether the fire can actually occur. Natural ignition source I_N depends on cloud-to-ground lightning (CoGL), which is simulated by ModelE2 following the parameterization of Price and Rind (1994):

$$I_N = \mathrm{CoGL} = \begin{cases} 3.44 \times 10^{-5} \times H^{4.9} & \text{over land} \\ 6.4 \times 10^{-4} \times H^{1.73} & \text{over ocean} \end{cases} \quad (5)$$

where H is the cloud depth (unit: km). The number of anthropogenic ignition source I_A is calculated as follows:

$$I_A = k(\mathrm{PD}) \times \mathrm{PD} \times \alpha \quad (6)$$

where PD is population density (number/km^2), $k(\mathrm{PD}) = 6.8 \times \mathrm{PD}^{-0.6}$ stands for ignition potentials of human activity, and α is equal to 0.03. Human activities can also suppress fires,

https://doi.org/10.5194/acp-2022-175
Preprint. Discussion started: 4 April 2022

especially in highly populated area. The fraction of non-suppressed fires F_{NS} can be expressed as:

$$F_{NS} = c_1 + c_2 \times \exp(-\omega \times PD) \quad (7)$$

where c_1, c_2 and ω are constants and set to 0.05, 0.95 and 0.05, respectively.

With the calculation of flammability (Flam), ignition (I_N and I_A), and non-suppression (F_{NS}), the fire count density N_{fire} (unit: number/km^2) at a specific time step can be derived as:

$$N_{fire} = Flam \times (I_N + I_A) \times F_{NS} \quad (8)$$

Finally, fire emissions of trace gases and particulate matters FireEmis are calculated as:

$$FireEmis = N_{fire} \times EF \quad (9)$$

Here, EF is the PFT-specific emission factor of an air pollutant such as black carbon (BC), organic carbon (OC), NOx, CO, CH_4, Alkenes and Paraffin. For each pollutant species, simulated gridded emissions are grouped by dominant PFT and compared to GFED emissions over the same grids. The EF is then calibrated to minimize the root-mean-square error between the simulated and GFED data. Such calibration adjusts only the global total amount of fire emissions without changing the spatiotemporal pattern predicted by the parameterization.

2.4 Simulations

We perform four groups of sensitivity experiments (Table 1) with the ModelE2-YIBs model to quantify the fire-climate interactions through different radiative processes. The first group with suffix 'AD' considers only the ADE. The second (third) group with suffix 'AD_AI' ('AD_AA') considers both ADE and AIE (ADE and AAE). The fourth group with suffix 'AD_AI_AA' includes all three aerosol radiative effects (ADE, AIE, and AAE). Within each group, two runs are performed with (YF) or without (NF) fire emissions. For YF simulations, fire-induced aerosols are dynamically calculated based on fire emissions and atmospheric transport. These fire aerosols cause radiative perturbations and the consequent changes in climatic variables, which feedback to influence fire emissions. For NF simulations, fire emissions at each step are set to zero. By comparing the climatic variables from the YF and NF runs in the first group, we isolate the impacts of fire aerosols on climate through ADE. By comparing the climatic effects from the first and second (third) groups, we isolate the AIE (AAE) of fire aerosols. By comparing the climatic variables from YF and NF runs in the fourth group, the overall effect (ADE+AIE+AAE) is obtained.

For each simulation, CO_2 concentrations, SST/SIC, and population density in the year 2000

https://doi.org/10.5194/acp-2022-175
Preprint. Discussion started: 4 April 2022

Atmospheric Chemistry and Physics Discussions

are used as boundary conditions to drive the model. Each simulation is integrated for 25 years with the first 5 years spinning up and the last 20 years averaged and analyzed. Student *t*-test is performed and the significant changes at $p < 0.1$ are analyzed. In this study, downward (upward) radiative fluxes are defined as positive (negative). Given that the model is driven by prescribed SST and SIC, only the rapid adjustments of atmospheric variables are taken into account and we mainly focus on climate changes over land grid.

3 Results

3.1 Model evaluation

Simulated fire emissions of BC and OC show hotspots in the tropics, such as Amazon, Sahel, central Africa, and Southeast Asia (Fig. S1). The large tropical fire emissions are related to abundant vegetation and/or distinct dry seasons. Compared to GFED4.1s data, ModelE2-YIBs slightly underestimates boreal fire emissions especially over northern Asia and North America. On the global scale, fire releases 1.85 Tg (1 Tg = 10^{12} g) C year^{-1} of BC and 16.8 Tg C year^{-1} of OC in ModelE2-YIBs, close to the 1.86 Tg C year^{-1} of BC and 16.4 Tg C year^{-1} of OC estimated by GFED4.1s. In general, ModelE2-YIBs reasonably captures the spatial distribution of fire emissions, with high spatial correlations of 0.67 ($p < 0.01$) for BC and 0.58 ($p < 0.01$) for OC, and low normalized mean biases of 0.6% for BC and 2.4% for OC against satellite-based observations.

3.2 Fire-induced radiative perturbations

Fig. S2 shows the fire-induced changes in Aerosol Optical Depth (AOD) at 550nm. Fire emissions largely enhance surface aerosols especially over tropical regions. Hotspots are located in southern Africa and South America with regional enhancement larger than 0.05. In addition, large enhancement is also found at boreal high latitudes (> 0.01). At the global scale, fires enhance AOD by 0.006 with 0.01 over land.

Fire aerosols cause large perturbations in net radiation at top of atmosphere (TOA). Globally, the net radiation at TOA decreases 0.565 W m^{-2} by fire aerosols (Fig. 1a). Regionally, negative changes are predicted over central Africa, western South America, western North America and the boreal high latitudes. Diagnosis shows that fire-induced AIE dominates the reduction of TOA flux with a global value of -0.44 W m^{-2} (Fig. 1c), accounting for 78% of the total effects by fire aerosols.

https://doi.org/10.5194/acp-2022-175
Preprint. Discussion started: 4 April 2022

Atmospheric Chemistry and Physics Discussions

The spatial correlation coefficient is 0.62 over land grids between the perturbations by all aerosol effects and that by AIE alone. Compared to AIE, the changes in TOA radiative fluxes are much smaller for fire ADE (-0.058 W m^{-2}, Fig. 1b) and AAE (-0.016 W m^{-2}, Fig. 1d) with limited perturbations on land.

At the surface, fire aerosols decrease net shortwave radiation up to 9 W m^{-2} in central Africa and 7 W m^{-2} in Amazon (Fig. 2a), where biomass burning emissions are most intense (Fig. S1). Such pattern is in general consistent with the changes of TOA fluxes (Fig. 1a), leading to an average reduction of -1.23 W m^{-2} in the shortwave radiation over global land. The fire-induced ADE alone reduces land surface shortwave radiation by 0.65 W m^{-2} with the maximum center in Amazon (Fig. S3a). As a comparison, the fire-induced AIE causes a smaller reduction of -0.55 W m^{-2} with the hotspot in central Africa (Fig. S3c). The net effect of AAE by fire aerosols is positive mainly because fire AAE reduces surface albedo and increase shortwave radiation over Tibetan Plateau, boreal high latitudes, and Australia (Fig. S3e). However, the magnitude of AAE is much smaller compared to that of ADE and AIE.

Changes in surface longwave radiation (Fig. 2b) are much smaller than those in shortwave radiation (Fig. 2a). Regionally, positive changes are predicted in the western U.S., eastern Amazon, and South Africa, where fire-induced surface cooling (Fig. 3a) decreases the upward longwave radiation. On the global scale, fire aerosols cause a decrease of 0.28 W m^{-2} in surface upward longwave radiation. The reductions in shortwave radiation are largely balanced by changes in heat fluxes at the surface, which shows an average decrease of 0.83 W m^{-2} in the upward fluxes over land grids (Fig. 2c). Fire ADE and AIE lead to reductions of 0.50 W m^{-2} and 0.43 W m^{-2} in surface upward heat fluxes, respectively (Fig. S3b and S3d). Changes in sensible heat account for 82.2 % of the changes in total heat reduction, much higher than the contributions of 17.8% by latent heat fluxes (Fig. S4). Regionally, the upward sensible heat decreases in the western U.S. and Amazon mainly due to fire ADE, while the upward latent heat decreases in central Africa mainly by fire AIE (Fig. S5).

3.3 Fire-induced climatic change

In response to the perturbations in radiative fluxes, land surface air temperature (TAS) decreases 0.061°C globally by fire aerosols (Fig. 3a). Such cooling is mainly located in western

U.S., Amazon, and boreal Asia, following the large reductions in shortwave radiation (Fig. 2a). Meanwhile, moderate warming is predicted at the high latitudes of both hemispheres especially over the areas covered with land ice such as Greenland and Antarctica. Sensitivity experiments show that both ADE (Fig. 4a) and AIE (Fig. 4c) of fire aerosols result in net cooling globally, with regional reductions of TAS over boreal Asia and North America. In contrast, the fire AAE causes increases of TAS over boreal Asia and North America (Fig. 4e), where the deposition of BC aerosols reduces surface albedo. Consequently, the fire AAE results in a global warming of 0.054°C, which in part offsets the cooling effects by the ADE and AIE of fire aerosols.

Meanwhile, global land precipitation decreases by 0.18 mm/month with great spatial heterogeneity (Fig. 3b). Decreased precipitation is predicted over central Africa, boreal North America, and eastern Siberia. In contrast, increased rainfall is predicted in western U.S., eastern Amazon, and northern Asia. The reduction of precipitation is mainly contributed by fire AIE, which reduces cloud droplet size and inhibits local rainfall in central Africa (Fig. 4d). Consequently, latent heat fluxes are reduced to compensate the rainfall deficit in central Africa (Fig. S4b).

3.4 Fire-climate interactions

The fire-aerosol-induced changes in precipitation, VPD, lightning, and LAI can feed back to affect fire emissions. However, these changes may have contrasting impacts on fire activities. For example, the aerosol-induced reduction of precipitation in central Africa (Fig. 3b) increases local VPD (Fig. 5a) and consequently causes more fire emissions. Meanwhile, such enhanced drought condition inhibits plant growth and decreases local LAI (Fig. 5c), which has negative impacts on fire emissions by reducing fuel density. Furthermore, the fire AIE inhibits the development of convective cloud, which limits cloud height and the number of cloud-to-ground lightning in central Africa (Fig. 5b), leading to reduced ignition sources and fire emissions.

To illustrate the joint the impacts of fire-aerosol-induced climatic change, we count the number out of the four factors contributing positive effects to fire emissions over land grids (Fig. 5d). The larger (smaller) number indicates higher possibility of increasing (decreasing) fire emissions. Most of areas show neutral number of 2, indicating offsetting effects of the changes in fire-prone factors. Only 13.5 % of land grids show numbers higher than 2 with sparse distribution. In contrast, 32.1 % of land grids show numbers smaller than 2, especially for the grids over Siberia and western U.S.

https://doi.org/10.5194/acp-2022-175
Preprint. Discussion started: 4 April 2022

Atmospheric Chemistry and Physics Discussions

where the increased rainfall (Fig. 3b) and decreased VPD (Fig. 5a) inhibit fire emissions. Furthermore, the regional reductions in lightning ignition or LAI promote the inhibition effects. As a result, fire emissions in YF_AD_AI_AA decrease by 31.0 Gg year^{-1} (1.7%) for BC and 493.6 Gg year^{-1} (2.9%) for OC compared to NF_AD_AI_AA in which fire emissions do not perturb climate (Fig. 6).

4 Conclusions and discussion

We used the chemistry-climate-vegetation coupled model ModelE2-YIBs to quantify fire-climate interactions through ADE, AIE, and AAE. Globally, fire aerosols decrease TOA net radiation by 0.565 W m^{-2}, dominated by the AIE over central Africa. Surface net solar radiation also exhibits widespread reductions especially over fire-prone areas with compensations from the decreased sensible and latent heat fluxes. Following the changes in radiation, surface air temperature decreases by 0.061°C and land precipitation decreases by 0.18 mm/month, albeit with regional inconsistencies. The surface cooling is dominated by fire ADE and AIE, while the drought tendency is mainly contributed by fire AIE with hotspots in central Africa. AAE also plays an important role by introducing warming tendency at the mid-to-high latitudes. The fire-induced climatic change further affect VPD, LAI, and lightning ignitions, leading to reductions in global fire emissions of BC by 2% and OC by 3%.

Our predicted reduction of 0.565 W m^{-2} in TOA radiation by fire aerosols is close to the estimate of -0.51 W m^{-2} reported by Jiang et al. (2016) and -0.59 W m^{-2} of Zou et al. (2020) using different models with prescribed SST/SIC and fire-induced ADE, AIE and AAE (Table 2). Within such change, fire ADE alone makes a moderate contribution of -0.06 W m^{-2}, falling within the range of -0.2 to 0.2 W m^{-2} from other studies. The large uncertainty of fire ADE is likely related to the discrepancies in the BC absorption among climate models, which cause varied net effects when offsetting the radiative perturbations of scattering aerosols. As a comparison, fire AIE in our model induces a significant radiative effect of -0.44 W m^{-2}. However, such magnitude is much smaller than previous estimates of -0.7 to -1.1 W m^{-2} using different models (Table 2). We further estimated a limited fire AAE of -0.02 W m^{-2}, consistent with previous findings showing insignificant role of AAE by fire aerosols (Ward et al., 2012; Jiang et al., 2016). Our estimates of reductions in TAS and precipitation also fall within the range of previous studies (Table 2).

Our estimates are subject to some limitations and uncertainties. First, we considered only the fast climatic responses of land surface with prescribed SST and SIC in the simulations. Although most of fire-induced AOD changes are located on land (Fig. S2), the air-ocean interactions may cause complex feedbacks to aerosol radiative effects (Jiang et al., 2020). Such feedback should be explored in the future studies with a coupled ocean model. Second, the nonlinear effects of different radiative processes may influence the attribution results. In this study, we isolate the effects of AIE and AAE by subtracting variables between different groups following the approaches by Bauer and Menon (2012). However, the additive perturbations from individual processes are not equal to the total perturbations with all processes in one simulation. For example, the sum of three processes causes changes of TOA radiation by -0.51 W m^{-2} (Figs 1b-1d), surface temperature by -0.037 °C (Figs 4a, 4c, 4e), and precipitation by -1.09 mm $month^{-1}$ (Figs 4b, 4d, 4f). These perturbations are weaker than the net effects of -0.57 W m^{-2} (Fig. 1a) in radiation and -0.061 °C in temperature (Fig. 3a), but much stronger than that of -0.18 mm $month^{-1}$ in precipitation (Fig. 3b) predicted by the simulation with all three processes. As a result, the nonlinear feedbacks among different radiative processes may magnify or offset the final climatic responses to fire aerosols.

Despite these limitations, we made the first attempt to assess the two-way interaction between fire emissions and climate. Our results show that fire-emitted aerosols cause negative effective radiative forcing (ERF) of -0.57 W m^{-2}, which is about 20% of the anthropogenic ERF due to the increased greenhouse gases and aerosols from 1950 to 2019 (Ipcc, 2021). Such fire ERF largely reduces surface air temperature and regional precipitation, leading to further changes in fire emissions. Although the reduction of -2% to -3% in fire emissions by the fire-climate interaction seems limited, such change is a result of several complex feedbacks that may exert offsetting effects. Furthermore, our simulations reveal a strong inhibition effect of fire aerosols on LAI in central Africa due to the aerosol-induced drought intensification. Such negative effects on ecosystems are inconsistent with previous estimates that showed certain fertilization effects by fire aerosols (Yue and Unger, 2018), mainly because the rainfall deficit overweighs the diffuse fertilization effects of aerosols. With likely more fires under global warming (Abatzoglou et al., 2019), our results suggested complex and uncertain perturbations by fire emissions to radiation, climate, and ecosystem through fire-climate interactions.

https://doi.org/10.5194/acp-2022-175
Preprint. Discussion started: 4 April 2022

Atmospheric Chemistry and Physics Discussions
Open Access

Acknowledgements

This research was supported by the National Key Research and Development Program of China (grant no. 2019YFA0606802).

Competing Interests

The authors declare that they have no conflict of interest.

Data availability

Hadley Centre Sea Ice and Sea Surface Temperature dataset were obtain from https://www.metoffice.gov.uk/hadobs/hadisst/. Population data could be downloaded form https://cmr.earthdata.nasa.gov/search/concepts/C1739468823-SEDAC.html. GFED data were obtained from https://daac.ornl.gov/VEGETATION/guides/fire_emissions_v4_R1.html.

https://doi.org/10.5194/acp-2022-175
Preprint. Discussion started: 4 April 2022

Reference:

Abatzoglou, J. T., Williams, A. P., and Barbero, R.: Global Emergence of Anthropogenic Climate Change in Fire Weather Indices, Geophysical Research Letters, 46, 326-336, 10.1029/2018gl080959, 2019.

Albrecht, B. A.: Aerosols, Cloud Microphysics, and Fractional Cloudiness, 245, 1227-1230, doi:10.1126/science.245.4923.1227, 1989.

Andela, N., Morton, D. C., Giglio, L., Chen, Y., van der Werf, G. R., Kasibhatla, P. S., DeFries, R. S., Collatz, G. J., Hantson, S., Kloster, S., Bachelet, D., Forrest, M., Lasslop, G., Li, F., Mangeon, S., Melton, J. R., Yue, C., and Randerson, J. T.: A human-driven decline in global burned area, Science, 356, 1356, 10.1126/science.aal4108, 2017.

Andreae, M. O., Rosenfeld, D., Artaxo, P., Costa, A. A., Frank, G. P., Longo, K. M., and Silva-Dias, M. A. F.: Smoking Rain Clouds over the Amazon, 303, 1337-1342, doi:10.1126/science.1092779, 2004.

Bali, K., Mishra, A. K., and Singh, S.: Impact of anomalous forest fire on aerosol radiative forcing and snow cover over Himalayan region, Atmospheric Environment, 150, 264-275, https://doi.org/10.1016/j.atmosenv.2016.11.061, 2017.

Bauer, S. E. and Menon, S.: Aerosol direct, indirect, semidirect, and surface albedo effects from sector contributions based on the IPCC AR5 emissions for preindustrial and present-day conditions, 117, https://doi.org/10.1029/2011JD016816, 2012.

Carslaw, K. S., Boucher, O., Spracklen, D. V., Mann, G. W., Rae, J. G. L., Woodward, S., and Kulmala, M.: A review of natural aerosol interactions and feedbacks within the Earth system, Atmos. Chem. Phys., 10, 1701-1737, 10.5194/acp-10-1701-2010, 2010.

Chen, G., Guo, Y., Yue, X., Tong, S., Gasparrini, A., Bell, M. L., Armstrong, B., Schwartz, J., Jaakkola, J. J. K., Zanobetti, A., Lavigne, E., Nascimento Saldiva, P. H., Kan, H., Royé, D., Milojevic, A., Overcenco, A., Urban, A., Schneider, A., Entezari, A., Vicedo-Cabrera, A. M., Zeka, A., Tobias, A., Nunes, B., Alahmad, B., Forsberg, B., Pan, S.-C., Íñiguez, C., Ameling, C., De la Cruz Valencia, C., Åström, C., Houthuijs, D., Van Dung, D., Samoli, E., Mayvaneh, F., Sera, F., Carrasco-Escobar, G., Lei, Y., Orru, H., Kim, H., Holobaca, I.-H., Kyselý, J., Teixeira, J. P., Madureira, J., Katsouyanni, K., Hurtado-Díaz, M., Maasikmets, M., Ragettli, M. S., Hashizume, M., Stafoggia, M., Pascal, M., Scortichini, M., de Sousa Zanotti Stagliorio Coêlho, M., Valdés Ortega, N., Ryti, N. R. I., Scovronick, N., Matus, P., Goodman, P., Garland, R. M., Abrutzky, R., Garcia, S. O., Rao, S., Fratianni, S., Dang, T. N., Colistro, V., Huber, V., Lee, W., Seposo, X., Honda, Y., Guo, Y. L., Ye, T., Yu, W., Abramson, M. J., Samet, J. M., and Li, S.: Mortality risk attributable to wildfire-related PM_{2·5} pollution: a global time series study in 749 locations, The Lancet Planetary Health, 5, e579-e587, 10.1016/S2542-5196(21)00200-X, 2021.

Flannigan, M. and Harrington, J. B.: A Study of the Relation of Meteorological Variables to Monthly Provincial Area Burned by Wildfire in Canada (1953–80), Journal of Applied Meteorology and Climatology, 27, 441-452, 10.1175/1520-0450(1988)027<0441:ASOTRO>2.0.CO;2, 1988.

Flannigan, M., Krawchuk, M. A., de Groot, W. J., Wotton, B. M., and Gowman, L. M.: Implications of changing climate for global wildland fire %J International Journal of Wildland Fire, 18, 483-507, https://doi.org/10.1071/WF08187, 2009.

Flannigan, M., Cantin, A. S., de Groot, W. J., Wotton, M., Newbery, A., and Gowman, L. M.: Global wildland fire season severity in the 21st century, Forest Ecology and Management, 294, 54-61, https://doi.org/10.1016/j.foreco.2012.10.022, 2013.

Friedlingstein, P., O'Sullivan, M., Jones, M. W., Andrew, R. M., Hauck, J., Olsen, A., Peters, G. P., Peters, W., Pongratz, J., Sitch, S., Le Quéré, C., Canadell, J. G., Ciais, P., Jackson, R. B., Alin, S., Aragão, L. E.

O. C., Arneth, A., Arora, V., Bates, N. R., Becker, M., Benoit-Cattin, A., Bittig, H. C., Bopp, L., Bultan, S., Chandra, N., Chevallier, F., Chini, L. P., Evans, W., Florentie, L., Forster, P. M., Gasser, T., Gehlen, M., Gilfillan, D., Gkritzalis, T., Gregor, L., Gruber, N., Harris, I., Hartung, K., Haverd, V., Houghton, R. A., Ilyina, T., Jain, A. K., Joetzjer, E., Kadono, K., Kato, E., Kitidis, V., Korsbakken, J. I., Landschützer, P., Lefèvre, N., Lenton, A., Lienert, S., Liu, Z., Lombardozzi, D., Marland, G., Metzl, N., Munro, D. R., Nabel, J. E. M. S., Nakaoka, S. I., Niwa, Y., O'Brien, K., Ono, T., Palmer, P. I., Pierrot, D., Poulter, B., Resplandy, L., Robertson, E., Rödenbeck, C., Schwinger, J., Séférian, R., Skjelvan, I., Smith, A. J. P., Sutton, A. J., Tanhua, T., Tans, P. P., Tian, H., Tilbrook, B., van der Werf, G., Vuichard, N., Walker, A. P., Wanninkhof, R., Watson, A. J., Willis, D., Wiltshire, A. J., Yuan, W., Yue, X., and Zaehle, S.: Global Carbon Budget 2020, Earth Syst. Sci. Data, 12, 3269-3340, 10.5194/essd-12-3269-2020, 2020.

Gao, J.: Downscaling Global Spatial Population Projections from 1/8-degree to 1-km Grid Cells, 2017.

Gao, J.: Global 1-km Downscaled Population Base Year and Projection Grids Based on the Shared Socioeconomic Pathways, Revision 01, NASA Socioeconomic Data and Applications Center (SEDAC) [dataset], 2020.

Giglio, L., Randerson, J. T., and van der Werf, G. R.: Analysis of daily, monthly, and annual burned area using the fourth-generation global fire emissions database (GFED4), Journal of Geophysical Research: Biogeosciences, 118, 317-328, https://doi.org/10.1002/jgrg.20042, 2013.

Grandey, B. S., Lee, H. H., and Wang, C.: Radiative effects of interannually varying vs. interannually invariant aerosol emissions from fires, Atmos. Chem. Phys., 16, 14495-14513, 10.5194/acp-16-14495-2016, 2016.

Hansen, J. and Nazarenko, L.: Soot climate forcing via snow and ice albedos, 101, 423-428, 10.1073/pnas.2237157100 %J Proceedings of the National Academy of Sciences of the United States of America, 2004.

Heald, C. L., Ridley, D. A., Kroll, J. H., Barrett, S. R. H., Cady-Pereira, K. E., Alvarado, M. J., and Holmes, C. D.: Contrasting the direct radiative effect and direct radiative forcing of aerosols, Atmos. Chem. Phys., 14, 5513-5527, 10.5194/acp-14-5513-2014, 2014.

Hudson, P. K., Murphy, D. M., Cziczo, D. J., Thomson, D. S., de Gouw, J. A., Warneke, C., Holloway, J., Jost, H.-J., and Hübler, G.: Biomass-burning particle measurements: Characteristic composition and chemical processing, 109, https://doi.org/10.1029/2003JD004398, 2004.

IPCC: Contribution of Working Groups I, II and III to the Fifth Assessment Report of the Intergovernmental Panel on Climate Change [Core Writing Team, R.K. Pachauri and L.A. Meyer (eds.)], IPCC, Geneva, Switzerland, 151 pp.2014.

IPCC: Climate Change 2021: The Physical Science Basis. Contribution of Working Group I to the Sixth Assessment Report of the Intergovernmental Panel on Climate Change [Masson-Delmotte, V., P. Zhai, A. Pirani, S. L. Connors, C. Péan, S. Berger, N. Caud, Y. Chen, L. Goldfarb, M. I. Gomis, M. Huang, K. Leitzell, E. Lonnoy, J. B. R. Matthews, T. K. Maycock, T. Waterfield, O. Yelekçi, R. Yu and B. Zhou (eds.)], Cambridge University Press.2021.

Jiang, Y., Lu, Z., Liu, X., Qian, Y., Zhang, K., Wang, Y., and Yang, X. Q.: Impacts of global open-fire aerosols on direct radiative, cloud and surface-albedo effects simulated with CAM5, Atmos. Chem. Phys., 16, 14805-14824, 10.5194/acp-16-14805-2016, 2016.

Jiang, Y., Yang, X.-Q., Liu, X., Qian, Y., Zhang, K., Wang, M., Li, F., Wang, Y., and Lu, Z.: Impacts of Wildfire Aerosols on Global Energy Budget and Climate: The Role of Climate Feedbacks, Journal of Climate, 33, 3351-3366, 10.1175/JCLI-D-19-0572.1, 2020.

Kang, S., Zhang, Y., Qian, Y., and Wang, H.: A review of black carbon in snow and ice and its impact on the cryosphere, Earth-Science Reviews, 210, 103346, https://doi.org/10.1016/j.earscirev.2020.103346, 2020.

Koch, D., Schmidt, G. A., and Field, C. V.: Sulfur, sea salt, and radionuclide aerosols in GISS ModelE, 111, https://doi.org/10.1029/2004JD005550, 2006.

Liu, J. C., Pereira, G., Uhl, S. A., Bravo, M. A., and Bell, M. L.: A systematic review of the physical health impacts from non-occupational exposure to wildfire smoke, Environmental Research, 136, 120-132, https://doi.org/10.1016/j.envres.2014.10.015, 2015.

Liu, Y., Goodrick, S., and Heilman, W.: Wildland fire emissions, carbon, and climate: Wildfire–climate interactions, Forest Ecology and Management, 317, 80-96, https://doi.org/10.1016/j.foreco.2013.02.020, 2014.

Macias Fauria, M. and Johnson, E. A.: Large-scale climatic patterns control large lightning fire occurrence in Canada and Alaska forest regions, Journal of Geophysical Research: Biogeosciences, 111, https://doi.org/10.1029/2006JG000181, 2006.

Menon, S., Koch, D., Beig, G., Sahu, S., Fasullo, J., and Orlikowski, D.: Black carbon aerosols and the third polar ice cap, Atmos. Chem. Phys., 10, 4559-4571, 10.5194/acp-10-4559-2010, 2010.

Menon, S., Del Genio, A. D., Kaufman, Y., Bennartz, R., Koch, D., Loeb, N., and Orlikowski, D.: Analyzing signatures of aerosol-cloud interactions from satellite retrievals and the GISS GCM to constrain the aerosol indirect effect, 113, https://doi.org/10.1029/2007JD009442, 2008.

Pechony, O. and Shindell, D. T.: Fire parameterization on a global scale, 114, https://doi.org/10.1029/2009JD011927, 2009.

Price, C. and Rind, D.: Modeling Global Lightning Distributions in a General Circulation Model, Monthly Weather Review, 122, 1930-1939, 10.1175/1520-0493(1994)122<1930:MGLDIA>2.0.CO;2, 1994.

Randerson, J. T., Chen, Y., van der Werf, G. R., Rogers, B. M., and Morton, D. C.: Global burned area and biomass burning emissions from small fires, Journal of Geophysical Research: Biogeosciences, 117, https://doi.org/10.1029/2012JG002128, 2012.

Rayner, N. A., Parker, D. E., Horton, E. B., Folland, C. K., Alexander, L. V., Rowell, D. P., Kent, E. C., and Kaplan, A.: Global analyses of sea surface temperature, sea ice, and night marine air temperature since the late nineteenth century, 108, https://doi.org/10.1029/2002JD002670, 2003.

Schmidt, G. A., Kelley, M., Nazarenko, L., Ruedy, R., Russell, G. L., Aleinov, I., Bauer, M., Bauer, S. E., Bhat, M. K., Bleck, R., Canuto, V., Chen, Y.-H., Cheng, Y., Clune, T. L., Del Genio, A., de Fainchtein, R., Faluvegi, G., Hansen, J. E., Healy, R. J., Kiang, N. Y., Koch, D., Lacis, A. A., LeGrande, A. N., Lerner, J., Lo, K. K., Matthews, E. E., Menon, S., Miller, R. L., Oinas, V., Oloso, A. O., Perlwitz, J. P., Puma, M. J., Putman, W. M., Rind, D., Romanou, A., Sato, M., Shindell, D. T., Sun, S., Syed, R. A., Tausnev, N., Tsigaridis, K., Unger, N., Voulgarakis, A., Yao, M.-S., and Zhang, J.: Configuration and assessment of the GISS ModelE2 contributions to the CMIP5 archive, Journal of Advances in Modeling Earth Systems, 6, 141-184, 10.1002/2013MS000265, 2014.

Twomey, S.: Pollution and the planetary albedo, Atmospheric Environment (1967), 8, 1251-1256, https://doi.org/10.1016/0004-6981(74)90004-3, 1974.

van der Werf, G. R., Randerson, J. T., Giglio, L., van Leeuwen, T. T., Chen, Y., Rogers, B. M., Mu, M., van Marle, M. J. E., Morton, D. C., Collatz, G. J., Yokelson, R. J., and Kasibhatla, P. S.: Global fire emissions estimates during 1997–2016, Earth Syst. Sci. Data, 9, 697-720, 10.5194/essd-9-697-2017, 2017.

Veira, A., Kloster, S., Schutgens, N. A. J., and Kaiser, J. W.: Fire emission heights in the climate system

https://doi.org/10.5194/acp-2022-175
Preprint. Discussion started: 4 April 2022

– Part 2: Impact on transport, black carbon concentrations and radiation, Atmos. Chem. Phys., 15, 7173-7193, 10.5194/acp-15-7173-2015, 2015.

Ward, D. S., Kloster, S., Mahowald, N. M., Rogers, B. M., Randerson, J. T., and Hess, P. G.: The changing radiative forcing of fires: global model estimates for past, present and future, Atmos. Chem. Phys., 12, 10857-10886, 10.5194/acp-12-10857-2012, 2012.

Warren, S. G. and Wiscombe, W. J.: A Model for the Spectral Albedo of Snow. II: Snow Containing Atmospheric Aerosols %J Journal of Atmospheric Sciences, 37, 2734-2745, 10.1175/1520-0469(1980)037<2734:Amftsa>2.0.Co;2, 1980.

Warren, S. G. and Wiscombe, W. J.: Dirty snow after nuclear war, Nature, 313, 467-470, 10.1038/313467a0, 1985.

Xu, L., Zhu, Q., Riley, W. J., Chen, Y., Wang, H., Ma, P.-L., and Randerson, J. T.: The Influence of Fire Aerosols on Surface Climate and Gross Primary Production in the Energy Exascale Earth System Model (E3SM), Journal of Climate, 34, 7219-7238, 10.1175/JCLI-D-21-0193.1, 2021.

Yu, P., Toon, O. B., Bardeen, C. G., Zhu, Y., Rosenlof, K. H., Portmann, R. W., Thornberry, T. D., Gao, R.-S., Davis, S. M., Wolf, E. T., Gouw, J. d., Peterson, D. A., Fromm, M. D., and Robock, A.: Black carbon lofts wildfire smoke high into the stratosphere to form a persistent plume, 365, 587-590, doi:10.1126/science.aax1748, 2019.

Yue, X. and Unger, N.: The Yale Interactive terrestrial Biosphere model version 1.0: description, evaluation and implementation into NASA GISS ModelE2, Geosci. Model Dev., 8, 2399-2417, 10.5194/gmd-8-2399-2015, 2015.

Yue, X. and Unger, N.: Fire air pollution reduces global terrestrial productivity, Nature Communications, 9, 5413, 10.1038/s41467-018-07921-4, 2018.

Yue, X., Strada, S., Unger, N., and Wang, A.: Future inhibition of ecosystem productivity by increasing wildfire pollution over boreal North America, Atmos. Chem. Phys., 17, 13699-13719, 10.5194/acp-17-13699-2017, 2017.

Zhuravleva, T. B., Kabanov, D. M., Nasrtdinov, I. M., Russkova, T. V., Sakerin, S. M., Smirnov, A., and Holben, B. N.: Radiative characteristics of aerosol during extreme fire event over Siberia in summer 2012, Atmos. Meas. Tech., 10, 179-198, 10.5194/amt-10-179-2017, 2017.

Zou, Y., Wang, Y., Qian, Y., Tian, H., Yang, J., and Alvarado, E.: Using CESM-RESFire to understand climate–fire–ecosystem interactions and the implications for decadal climate variability, Atmos. Chem. Phys., 20, 995-1020, 10.5194/acp-20-995-2020, 2020.

https://doi.org/10.5194/acp-2022-175
Preprint. Discussion started: 4 April 2022

Atmospheric Chemistry and Physics
Discussions

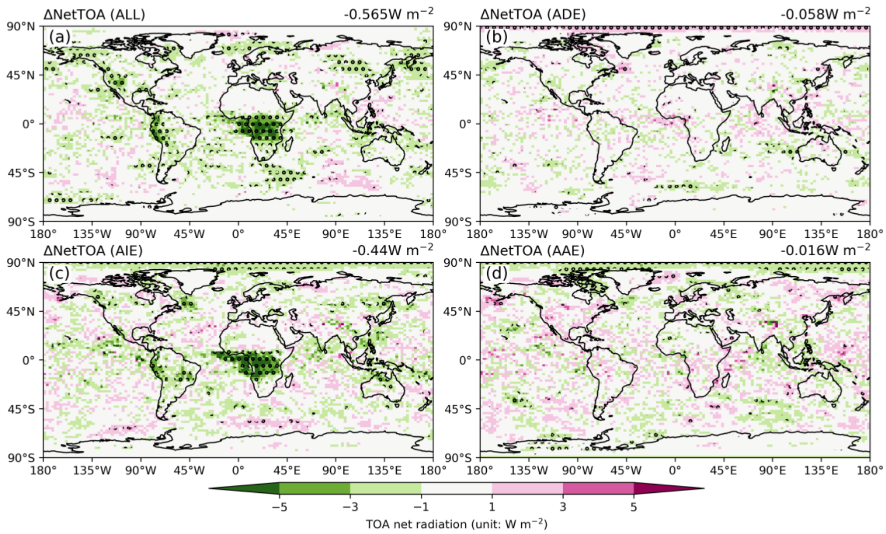

Fig. 1 Changes in net radiation flux at top of atmosphere due to (a) total effects, (b) ADE, (c)AIE, and (d) AAE of fire aerosols. Positive values represent the increase of downward radiation. Global average is shown at the top of each panel. Dots denote areas with significant ($p < 0.1$) changes.

https://doi.org/10.5194/acp-2022-175
Preprint. Discussion started: 4 April 2022

Atmospheric Chemistry and Physics
Discussions

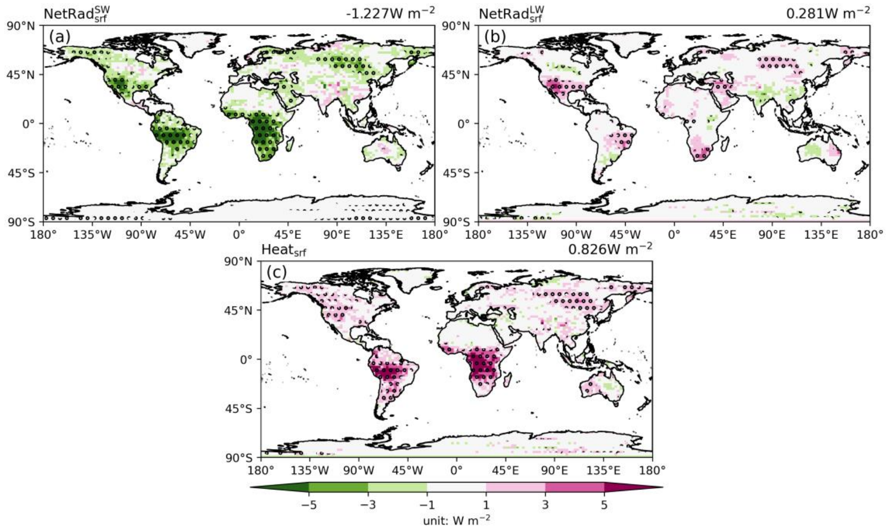

Fig. 2 Changes in surface net (a) shortwave radiation, (b) longwave radiation, and (c) heat flux (sensible + latent) over land grids caused by fire aerosols. Positive values represent the increase of downward radiation. Global average value is shown at the top of each panel. Dots denote areas with significant ($p < 0.1$) changes.

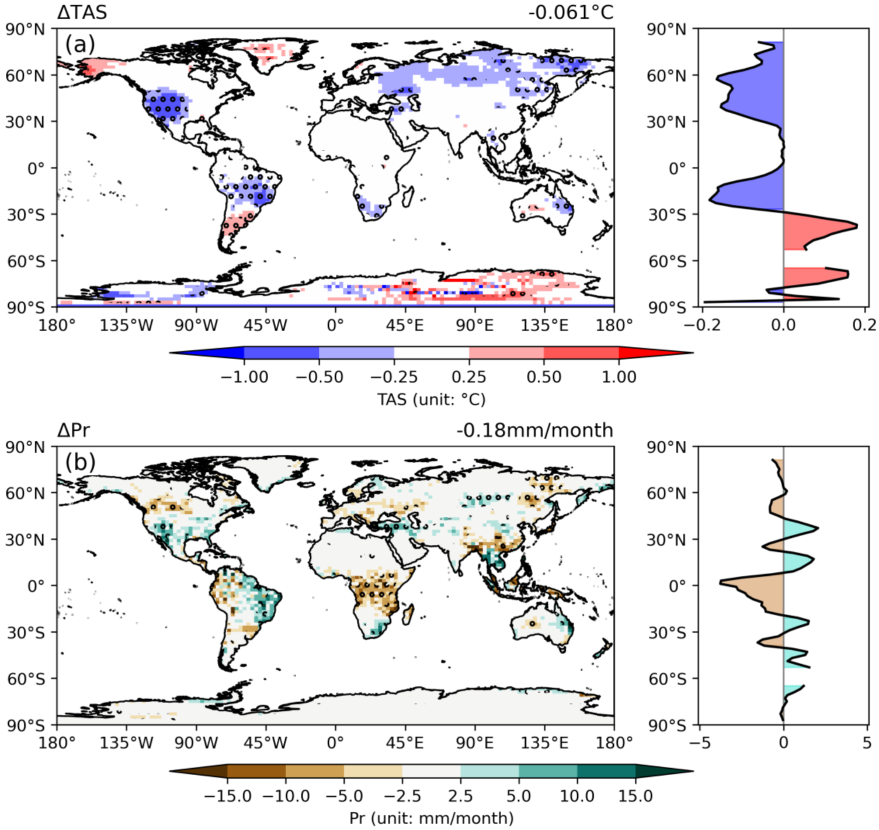

Fig. 3 Changes in (a) surface air temperature and (b) precipitation over land grids caused by fire aerosols. The zonal averages of these changes are shown by the side of each panel. Global average value (land average for precipitation) is shown at the top of each panel. Dots denote areas with significant ($p < 0.1$) changes.

https://doi.org/10.5194/acp-2022-175
Preprint. Discussion started: 4 April 2022

Atmospheric Chemistry and Physics Discussions
Open Access

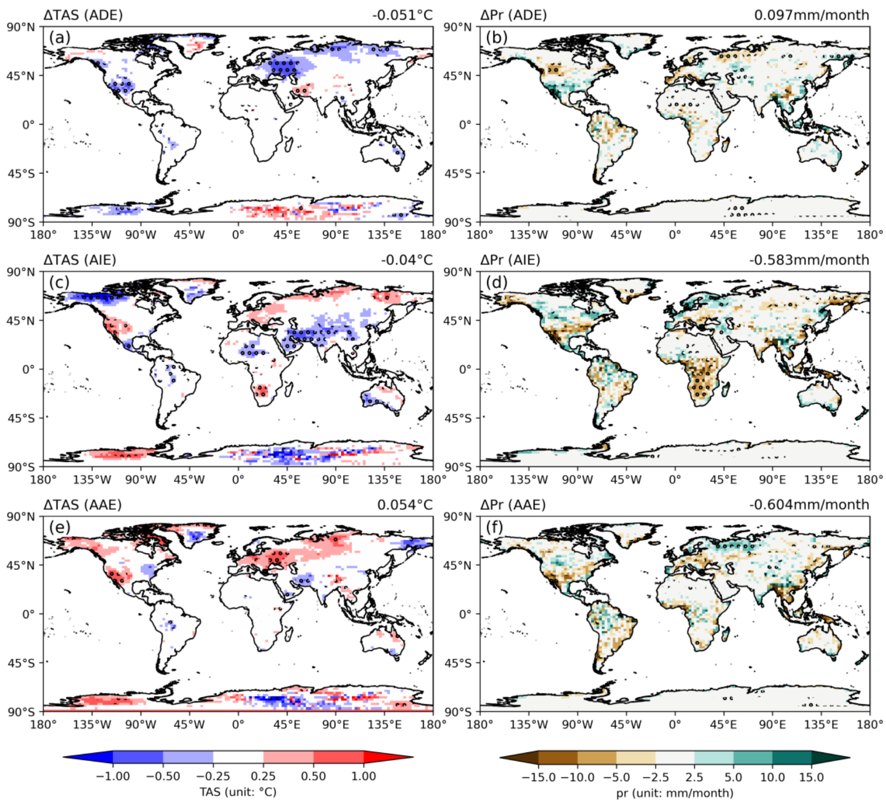

Fig. 4 Changes in (a, c, e) surface air temperature and (b, d, f) precipitation over land grids due to (a, b) ADE, (c, d)AIE, and (e, f) AAE of fire aerosols. Global average is shown at the top of each panel. Dots denote areas with significant ($p < 0.1$) changes.

https://doi.org/10.5194/acp-2022-175
Preprint. Discussion started: 4 April 2022

Atmospheric Chemistry and Physics
Open Access
Discussions

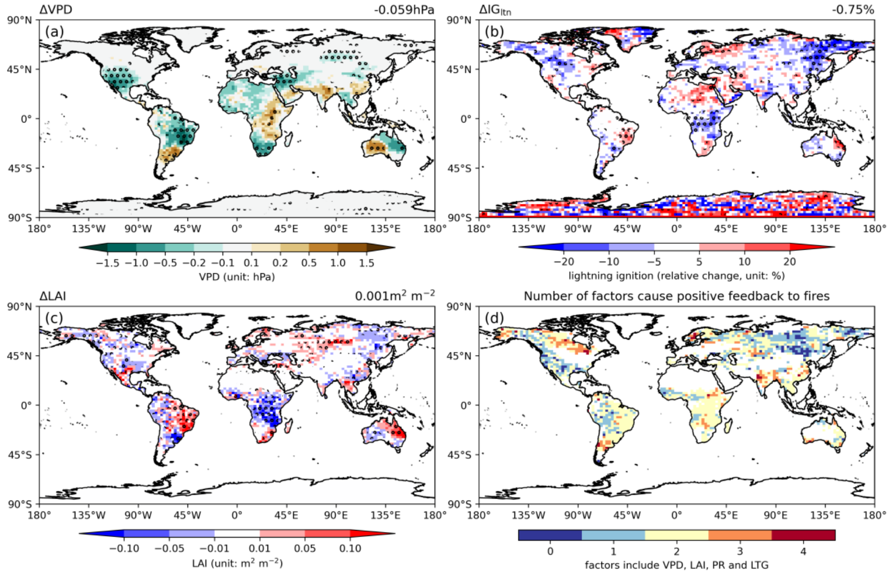

Fig. 5 Changes in (a) vapor pressure deficit (VPD), (b) lightning ignition, and (c) leaf area index (LAI) over land grids induced by fire aerosols. Global land average value is shown at the top of each panel. Dots denote areas with significant (p < 0.1) changes. The number of factors whose changes induced by fire aerosols cause positive feedback to fire emissions is shown in (d). Only grids with fire-emitted OC larger than 1×10^{-12} kg s^{-1} m^{-2} are shown in (d).

https://doi.org/10.5194/acp-2022-175
Preprint. Discussion started: 4 April 2022

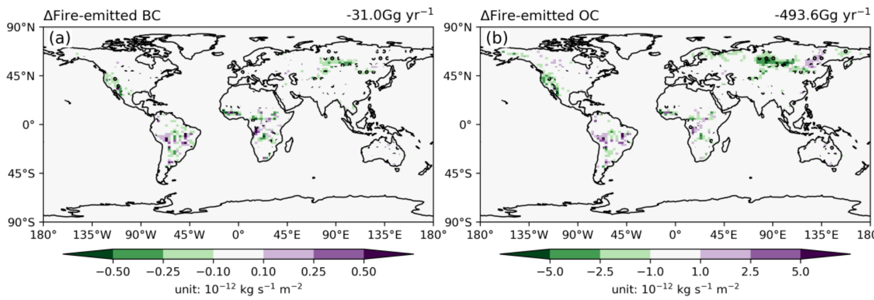

Fig. 6 Changes in fire emissions of (a) BC and (b) OC through fire-climate interactions. The changes of fire emissions are calculated as the differences between YF_AD_AI_AA and NF_AD_AI_AA with dots indicating significant ($p < 0.1$) changes.

https://doi.org/10.5194/acp-2022-175
Preprint. Discussion started: 4 April 2022

Atmospheric Chemistry and Physics Discussions

Table 1. Summary of simulations using ModelE2-YIBs

Simulation	Fires [a]	Aerosol direct effect	Aerosol indirect effect	Aerosol albedo effect
NF_AD	No	Yes	No	No
YF_AD	Yes	Yes	No	No
NF_AD_AI	No	Yes	Yes	No
YF_AD_AI	Yes	Yes	Yes	No
NF_AD_AA	No	Yes	No	Yes
YF_AD_AA	Yes	Yes	No	Yes
NF_AD_AI_AA	No	Yes	Yes	Yes
YF_AD_AI_AA	Yes	Yes	Yes	Yes

[a] All simulations predict fire emissions but the runs with NF do not feed the fire aerosols into the model to perturb radiative fluxes.

https://doi.org/10.5194/acp-2022-175
Preprint. Discussion started: 4 April 2022

Table 2. Comparsion of the simulated fire-induced change in radiative forcings at TOA and surface climate with previous studies

Reference	RF ($W\ m^{-2}$)	ADE ($W\ m^{-2}$)	AIE ($W\ m^{-2}$)	AAE ($W\ m^{-2}$)	TAS (°C)	Pr ($mm\ month^{-1}$)
Ward et al. (2012)[a]	-0.55	0.10	-1.00	0.00	—	—
Heald et al. (2014)	—	-0.19	—	—	—	—
Veira et al. (2015)	—	-0.20	—	—	—	—
Grandey et al. (2016)	-1.0	0.04	-1.11	-0.1	—	-0.018
Jiang et al. (2016)	-0.51	0.16	-0.70	0.03	-0.03	-0.3
Zou et al. (2020)	-0.59	-0.003	-0.82	0.19	—	—
Xu et al. (2021)	-0.73	0.25	-0.98	—	-0.17	-1.2
This study	-0.565	-0.058	-0.440	-0.016	-0.061	-0.18

[a] other effects of fire-induced on radiative turbulances are considered in this paper